IMAGING OF FLAME FRONTS BY FLUORESCENCE OF HYDROXYL RADICALS: A FRACTAL APPROACH FOR THE DETERMINATION OF FRONT POSITION

G. Troiani, M. Marrocco
guido.troiani@enea.it
ENEA C.R. Casaccia, Sustainable Combustion Laboratory, Rome, Italy

Abstract
Surfaces of maximum heat release (flame fronts) attract much attention for their physical and chemical importance in combustion processes. Their conventional analysis based on imaging of OH fluorescence is here scrutinized from the perspective of fractal concepts. These can be used to strengthen the idea according to which the signal isosurface that better correlates with the position of the maximum fluorescence gradient shows strong correspondence with the surface of maximum heat release. The findings are supported by experiments and simulations.

Introduction
Optical spectroscopy is fundamental to the interdisciplinary understanding of combustion where the interplay of thermodynamics, chemical kinetics, fluid mechanics and transport phenomena poses serious and multi-faceted issues to be dealt with [1]. To this end, laser spectroscopic techniques are employed in premixed combustion to gain information about thin reactive surfaces, otherwise known as flame fronts, separating the reactant mixture from the burned products [2]. In this regard, one of the most common equipments to study the connection between mass transport and chemistry across the flame front combines the experimental arrangements for Particle Image Velocimetry (PIV) and Laser Induced Fluorescence (LIF). The former is based on Mie scattering from solid particles that are seeded into the main gas flow. The latter is used to image fluorescence from suitable combustion intermediates such as radicals (OH, CH, etc.) that are regarded as fundamental chemical markers of the dominant reactions taking place across the flame front [3].
The spatial definition of the flame front, however, is subject to a certain arbitrariness depending on the observable chosen for the front detection. Now, assuming the thermal layer as reference [2], the key point is to quantify the spatial shift and other geometrical characteristics of the flame front arising from the choice of one observable rather than another. This research is laid out in recent works, where it is established that the choice of different variables to probe flame fronts, e.g. temperature by LRS (Linear Rayleigh Scattering), hydroxyl concentration by OH-LIF, particle distribution by CPIV (Conditional Particle Image Velocimetry),

does not substantially affect average quantities such as the mean progress variable distribution [4]. By contrast, dealing with fine scale statistics, the multiscale nature of turbulence is also reflected on its mutual interaction with combustion phenomena. Examples are the scale dependence of turbulent combustion velocity [5] and the fractal scaling of flame fronts. This effect is more intense near the preheat zone of the flame front where turbulent velocity fluctuations and strain rates of suitable length scales [6] can alter and increase the temperature by enhanced transport of heat and species from the reaction zone [7].The result is a variety of isosurfaces contained between the preheat and the reaction zone, each of those with different surface wrinkling and curvature probability density function (PDF) [8]. In addition, the flame surface density Σ, defined in terms of the amount of wrinkled surface area contained in a probing volume, is commonly used for the modeling of the overall reaction rate [9], hence an accurate definition of the reference surface – as close as possible to the inner layer – is of crucial importance.
In this work, in order to analyze the reliability of front position studied by means of hydroxyl fluorescence, measurements of the OH fluorescence signal are performed in a turbulent premixed annular Bunsen burner fed with air/methane mixture. The instantaneous flame front is defined by the isoline of a suitable threshold level that better correlates with the maximum OH-fluorescence gradient [10] and thereafter other thresholds are chosen to simulate shifts of front position towards unburned/burned regions. The resulting fronts are finally analyzed in terms of scale-by-scale wrinkling characteristics emerging from fractal theory [11].

OH fluorescence measurements

The experimental set-up consists of an annular inlet bluff-body stabilized burner fed with a homogeneous mixture of methane and air at different equivalence ratios Φ. The Reynolds number, based on the bulk velocity and nozzle equivalent diameter of 25 mm, is maintained constant at a value of Re =10000 in order to assure a fully developed turbulent jet. The flame is anchored to the burner exit by the recirculation of hot products downstream the bluff-body. Four different flames are realized by changing the equivalence ratio, Φ = 0.67, 0.80, 1.03, 1.12. More details about the flames can be found in [10].
Flame front detection is performed by the acquisition of fluorescence signal emitted by OH radicals. To that end, a Nd:YAG laser beam is delivered through a tunable dye laser coupled with a second-harmonic generator crystal in order to shift the laser wavelength from 532 nm down to 282.93 nm, corresponding to the Q1 (6) absorption line of OH. A suitable cylindrical lens expands the beam into a 350 μm thick laser sheet. The resulting OH fluorescence emission is around 309 nm and is then collected by a 1024 ×1024 pixels ICCD (2 × 2 pixel binning) equipped with a 78 mm Nikon quartz lens, resulting in a map of 512 × 512 equivalent pixels with a resolution of 160 μm for each equivalent pixel. Furthermore, a narrow pass-band filter, 10 nm wide and centered at 310 nm, isolates the relevant spectral line.
The fluorescence signal from OH radical is proportional to its concentration and

relative measurements are possible (absolute measurements of concentrations are instead prevented from non-radiative disexcitation channels that are generally active together with detectable fluorescence emission). These indicate that the fluorescence signal rises abruptly across the flame front, where the OH radicals are formed, and then decreases more smoothly, within the product region. The explanation resides in the fact that, within the products, OH radicals disappear at a much slower rate than that characterizing their formation in the flame. This asymmetric behavior can be used to distinguish reactants from products, hence unveiling front position.
In fact, even though in our measurements the signal-to-noise ratio is usually sufficiently large (see figure (2), left panel, for signal-to-noise ratio level), the gradient field may suffer from significant high-frequency contamination. All the same, the signal may be smoothed by suitable filtering techniques, e.g. the non linear filter described in [12], which provides satisfactory results in this case. Nonetheless, a variant of the threshold method [13] is adopted, which locates the front by the isoline that better correlates with the maximum gradient in the region of interest.

Fractal analysis of isosurfaces

The multiscale nature of surfaces in fluid mechanics is suitable for the application of geometrical concepts of fractal theory to describe the amount of wrinkling. This follows from the fact that, when the surface is measured at successive –finer– resolution, the area increases with the resolution adopted. In particular, the surface increment follows a power law with a non-integer exponent, i.e., flame fronts are fractal objects. From a pure geometrical point of view, the surface area should diverge indefinitely with the resolution, but natural surfaces, among which flame fronts are not an exception, agree with this exponential scaling only in a finite range of scales, between the extremes called inner and *outer cut-offs* and are termed prefractals [11]. Within this context, when a box-counting technique is adopted [14], a power law exists for the number of boxes needed to cover the fractal object

$$N(\epsilon) \propto \epsilon^{-D_2} \quad , (1)$$

where ϱ is the box size and D_2 is the fractal dimension of the object embedded in a two-dimensional space. This suggests that, in our case of front analysis, the dimension of the whole three-dimensional flame front is $D = D_2 + 1$ [15].
Fractal scaling of the kind of equation (1) for non-reactive flows has been studied and, in some circumstances, analytical results have provided fractal dimensions which have also been corroborated by experiments. This is the case of perfectly passive scalar or turbulent/non-turbulent isosurfaces whose fractal dimension is shown to be 7/3 under the hypothesis of the existence of a thin viscous surface (viscous superlayer) separating the scalar (turbulent) from the outer space

(non-turbulent). With the further hypothesis of an intermittent kinetic energy dissipation field, the fractal dimension reaches the value of 2.37 [16].
In turbulent combustion, the inner structure of isosurfaces of flame fronts are dominated by viscosity, typical of the non-reactive fronts mentioned above, but now the system is additionally perturbed by front propagation at velocity S_L, i.e., the laminar burning velocity. For this reason, unlike passive scalars, flame front dynamics is not supported by exact results. Nevertheless, recent evidence suggests its possible prefractal structure [17], i.e., the scaling of equation (1) holds for a finite range of scales. Experiments also show that flame surfaces are less space-filling with fractal dimensions on the order of 2.10÷2.25 [18].
In our case, the object is given by a two dimensional cut of the flamelet surface that is represented by the fractal dimension D_2 in a range of scales confined between the inner (ϵ_i) and the outer (ϵ_o) cut-off. Fractal characteristics have been evaluated by the box-counting technique, which consists in enumerating the squared boxes of size ϱ necessary to entirely cover the whole object that, in this instance, is the contour of the flame front. A representative result is given in figure (1) where the average number of boxes $N(\varrho) = \frac{1}{\mathcal{N}} \sum_{l=1}^{\mathcal{N}} N_l(\epsilon)$ of scale ϱ necessary to cover the front is reported ($\mathcal{N}$ = 50 is the number of front images used to obtain an average value of N). Error bars in the figure represent the standard deviation $\sigma_N(\epsilon)$.
It is clear that a wide range of constant scaling does exist and it is lost at large and small scales, emphasizing the prefractal nature of fronts. The angular coefficient of the linear regression of data in a log-log plot allows for the determination of the fractal dimension.

Results

In previous sections, different observables – temperature, radicals, tracer distribution – along with different criteria (such as maximum gradient or maximum value) are discussed with the aim of extracting front position. As a further insight, the scale invariant characteristic of fractal dimensions can play the role of benchmark against which a front surface can be accepted as a flame front. To this purpose, different isosurfaces will be extracted from OH fluorescence measurements. The left panel of figure (2) shows the behavior of the fluorescence signal across a cut of one image collected by the ICCD. In agreement with what stated above, the fact that the signal raises quickly through the flame front, should assure a certain degree of freedom in the choice of the threshold level. It is also evident in the figure that an uncertainty of 67% in fluorescence level can shift the front position of about 1 mm, which is a value on the same order of the thermal front thickness. Again in the figure, different threshold levels (horizontal lines) correspond to different isosurfaces which appear to be inside or very close to the thermal layer. The resulting isolines of fluorescence signal are reported in the right panel of the same figure. Those ranging between 3500 and 5000 a.u. (arbitrary units) are spatially very close to each other; more specifically, they all lie within a layer whose thickness is on the order of 1 ÷ 1.5 mm, and, at first glance, their

degree of wrinkling seems quite similar to each other. Conversely, the isoline at 3000 a.u. appears rather different from the others, and it has been included in the analysis with the aim of showing substantially different statistical characteristics emerging from the comparison among the isosurfaces. These are determined by threshold levels ranging between 3000 and 5000 a.u. with steps of 500. The corresponding fractal dimensions are reported in figure (3). It is interesting to note that the results are grouped in two classes: isosurfaces relative to levels 4000, 4500 and 5000 a.u. display values that are known to be typical of flame fronts with $D_2 \in [1.1, 1.25]$. The reason for this grouping should be found in the fact that the selected isolevels are enclosed in a very narrow layer within the thermal layer, hence they all present the same statistical behavior. Fractal values coming from the isolevel of 3000 a.u. are instead aligned around the value of $D_2 = 1.37$. This result is quite interesting, since it suggests that the selected isosurface is much more similar to a passive scalar surface rather than to a flame front. This could lead to the conclusion that such surface does not belong to a flame front, but probably lies in the early zone of preheat of the thermal flame front [2] where thermal expansion is not yet the leading effect. In the end, the isolevel at 3500 a.u. seems to be a transition level with some values belonging to the first class of results and others to the second class.

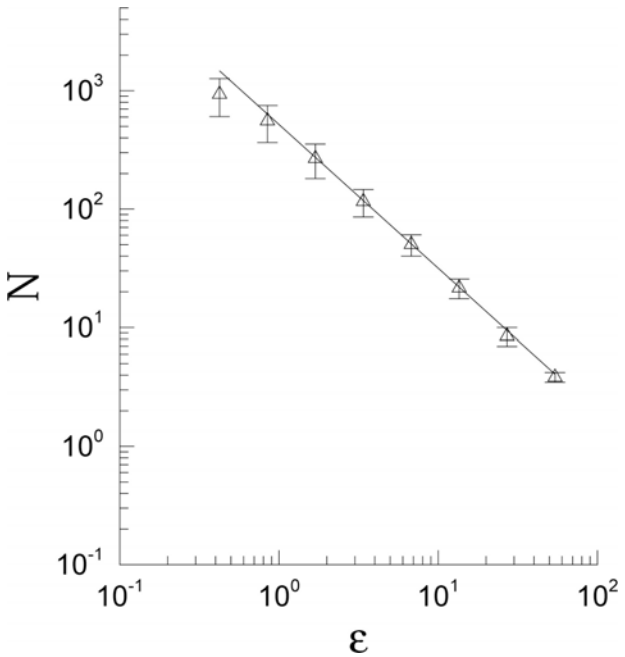

Figure 1. Fractal scaling for a flamelet front section of methane/air mixture with equivalence ration $\Phi = 1.03$. N is the number of boxes of scale ϵ necessary to cover the front. Error bars represent standard deviations $\sigma_N(\epsilon)$. $\epsilon = r/\delta_T$, with r the physical width of boxes, $\delta_T = 0.34$ mm.

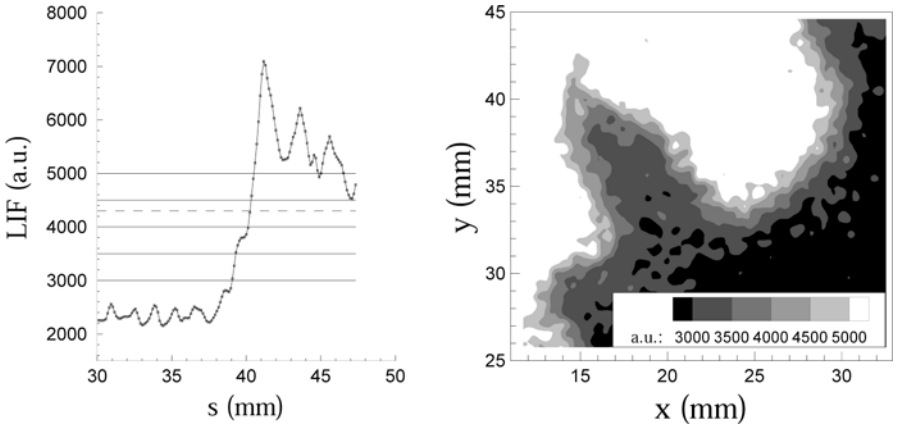

Figure 2. Left: OH fluorescence signal, Φ =1.03. Dashed line corresponds to maximum gradient position. Abscissa s originates at a point arbitrarily chosen in the reactants and crosses the flame front normally towards combustion products. Right: OH fluorescence map, Φ =1.03. Gray levels refer to different OH threshold values, as reported in the legend.

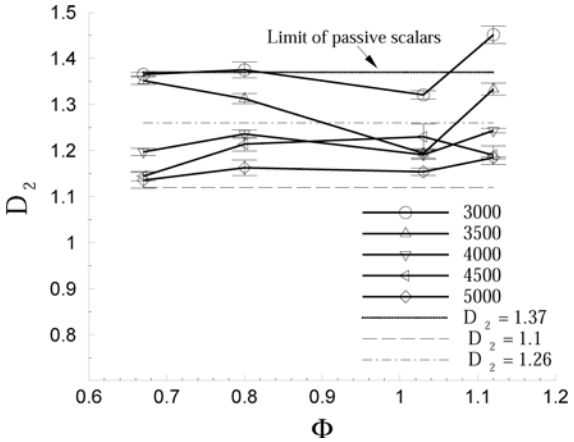

Figure 3. Fractal dimensions at different threshold levels.

Conclusion

In this work wrinkling characteristics of isosurfaces determined experimentally are studied by means of fractal analysis. The current research focuses on reliability of OH LIF with respect to its potential for imaging of flame fronts. In detail, fluorescence from hydroxyl radical is initially examined in comparison with the conventional definition of flame front known as the surface of maximum heat release. This confirms that the criterion of best correlation between the mere OH concentration and its maximum gradient establishes a valid strategy to isolate flame fronts among experimental data. The criterion has been applied to

measurements realized in a turbulent annular Bunsen flame operated under different conditions. The images have been elaborated with different signal thresholds to highlight the corresponding fractal behaviors of the resulting isosurfaces, which are exemplified in the right panel of figure (2). Finally, based on the measured fractal dimension, it is concluded that the wrinkling characteristics of the chosen fronts agree generally with each other except for those whose selecting thresholds are such that the limit of passive scalar is reached (figure (3)).

References

[1] J. Wolfrum, Lasers in combustion: from basic theory to practical devices, in: Symposium International On Combustion, Vol. 1, Combustion Institute, 1998, pp. 1–42.

[2] N. Peters, Turbulent combustion, Cambridge University Press, 2000.

[3] G. Hartung, J. Hult, R. Balachandran, M. R. Mackley, C. F. Kaminski, Flame front tracking in turbulent lean premixed flames using stereo PIV and time-sequenced planar LIF of OH, Applied Physics B: Lasers and Optics 96 (4) (2009) 843–862.

[4] S. Pfadler, A. Leipertz, F. Dinkelacker, Systematic experiments on turbulent premixed Bunsen flames including turbulent flux measurements, Combustion and Flame 152 (4) (2008) 616–631.

[5] N. Peters, The turbulent burning velocity for large-scale and small-scale turbulence, Journal of Fluid Mechanics 384 (1999) 107–132.

[6] J.F. Driscoll, Turbulent premixed combustion: Flamelet structure and its effect on turbulent burning velocities, Progress in Energy and Combustion Science 34 (1) (2008) 91–134.

[7] C. Kortschik, T. Plessing, N. Peters, Laser optical investigation of turbulent transport of temperature ahead of the preheat zone in a premixed flame, Combustion and Flame 136 (1-2) (2004) 43–50.

[8] N. Chakraborty, Comparison of displacement speed statistics of turbulent premixed flames in the regimes representing combustion in corrugated flamelets and thin reaction zones, Physics of Fluids 19 (10) (2007) 5109.

[9] K. N. C. Bray, C. R. S., in: Proc. Royal Soc. London A, Vol. 434, 1991, pp. 217–240.

[10] G. Troiani, M. Marrocco, S. Giammartini, C. Casciola, Counter-gradient transport in the combustion of a premixed CH4/air annular jet by combined PIV/OH-LIF, Combustion and Flame 156 (3) (2009) 608–620.

[11] B.B. Mandelbrot, The fractal geometry of nature, Wh Freeman, 1982.

[12] P. Perona, J. Malik, Scale-space and edge detection using anisotropic diffusion, IEEE Transactions on pattern Analysis and machine intelligence 12 (7) (1990) 629–639.

[13] P.A.M. Kalt, Y.C. Chen, R.W. Bilger, Experimental investigation of turbulent scalar flux in premixed stagnation-type flames, Combustion and Flame 129 (4) (2002) 401–415.

[14] K. Falconer, Fractal Geometry: Mathematical Foundations and Applications, John Wiley, 2003.
[15] K.R. Sreenivasan, C. Meneveau, The fractal facets of turbulence, Journal of Fluid Mechanics 173 (1986) 357–386.
[16] K.R. Sreenivasan, R. Ramshankar, C. Meneveau, Mixing, entrainment and fractal dimensions of surfaces in turbulent flows, Proceedings of the Royal Society of London. Series A, Mathematical and Physical Sciences (1989) 79–108.
[17] P. Meakin, Fractals, scaling and growth far from equilibrium, Cambridge Univ Pr, 1998.
[18] F.C. Gouldin, An application of fractals to modeling premixed turbulent flames, Combustion and flame 68 (3) (1987) 249–266.

10.4405/34proci2011.I13